Usefulness of image morphing techniques in cancer treatment by conformal radiotherapy

Hussein ATOUI[a], David SARRUT[b], Serge MIGUET[c]

[a]INSERM ERM107, 28 avenue du Doyen Lepine, 69394 Lyon Cedex 03, France
[b]Centre Léon Bérard, 28 rue Laënnec, 69373 Lyon Cedex 08, France
[c]Laboratoire LIRIS, 5 Avenue Pierre Mendès-France, 69676 Bron Cedex, France

Abstract Conformal radiotherapy is a cancer treatment technique, that targets high-energy X-rays to tumors with minimal exposure to surrounding healthy tissues. Irradiation ballistics is calculated based on an initial 3D Computerized Tomography (CT) scan. At every treatment session, the random positioning of the patient, compared to the reference position defined by the initial 3D CT scan, can generate treatment inaccuracies. Positioning errors potentially predispose to dangerous exposure to healthy tissues as well as insufficient irradiation to the tumor. A proposed solution would be the use of portal images generated by Electronic Portal Imaging Devices (EPID). Portal images (PI) allow a comparison with reference images retained by physicians, namely Digitally Reconstructed Radiographs (DRRs). At present, physicians must estimate patient positional errors by visual inspection. However, this may be inaccurate and consumes time. The automation of this task has been the subject of many researches. Unfortunately, the intensive use of DRRs and the high computing time required have prevented real time implementation. We are currently investigating a new method for DRR generation that calculates intermediate DRRs by 2D deformation of previously computed DRRs. We approach this investigation with the use of a morphing-based technique named mesh warping.

Keywords Image Registration, Conformal Radiotherapy, Digitally Reconstructed Radiographs, Image Morphing, Mesh Warping, Block Matching.

1. MEDICAL CONTEXT

This work was performed in collaboration with physicians from Lyons Léon Bérard Cancer Institute (France). Conformal radiotherapy is known to be a reliable technique for the treatment of cancer. Radiation is a powerful tool for cancer treatment based on the use of X-rays selectively targeted to destroy cancer cells. Conformal radiotherapy combines sophisticated current technologies allowing the precise anatomical definition and targeting of tumors, as well as the elaboration of dosage goals with input from CT facilities.

In theory, this technology makes it possible to deliver escalating X-ray doses with minimal exposure to surrounding healthy tissues. The main challenge is, however, to ensure accurate patient positioning so that the position of the patient at initial CT scan acquisition is reproducible throughout the treatment session.

Numerous studies[1] have shown that an inaccurate targeting might lead to a falsified and futile therapeutic result. One of the solutions proposed to reduce positioning errors is to use EPID images[2] (cf. Fig 1). Portal Images (PI) are projective images acquired before the beginning of each treatment session. They can be compared with reference images retained by physicians. The use of Digitally Reconstructed Radiographs (DRRs) is one of the techniques primarily used by physicians that generates 2D images by projection of the 3D CT scan image. At present, physicians have to accurately estimate patient positioning errors by visual inspection only. However, this is likely to be responsible for limited accuracy and unnecessary loss of time.

Further author information: (Send correspondence to Hussein ATOUI)
E-mail: hussein_atoui@hotmail.com, Telephone: +33 (0)4 72 35 76 71

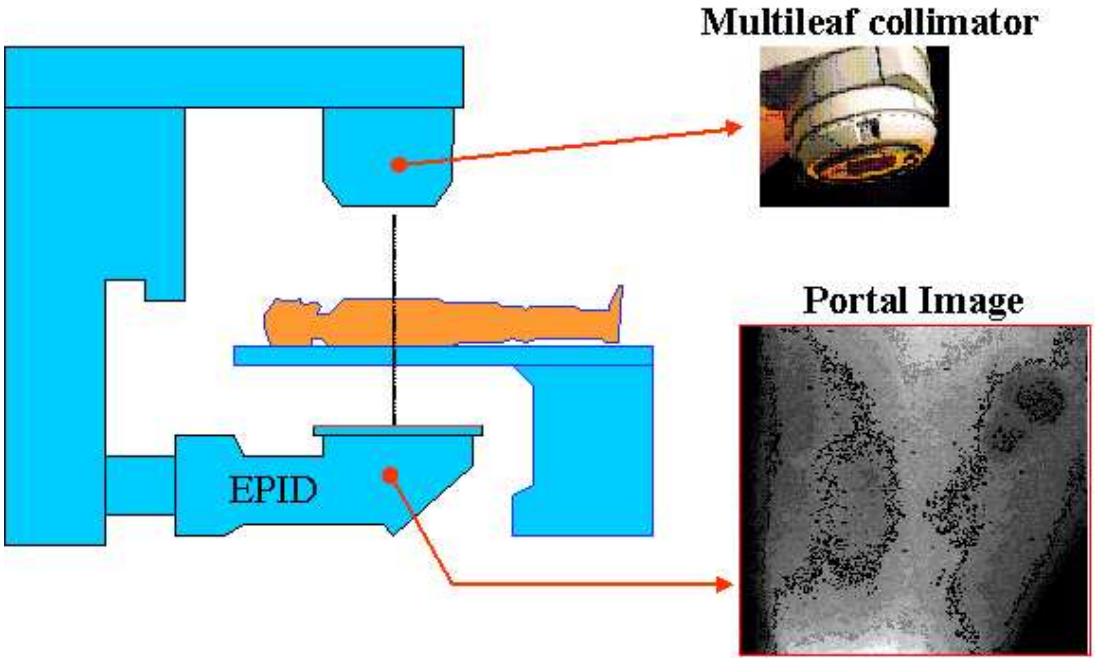

Figure 1. EPID

An automatic method to evaluate setup errors was thus developed. Details are given in the following section. Section 3 describes the optimization of the method involved through the acceleration of the DRR generation phase, whereas experiments and results are given in section 4.

2. INTENSITY-BASED 2D/3D REGISTRATION

2.1. Background

Several image registration methods have been used to compare portal images with the reference image (CT) as illustrated in figure 2. *Sarrut et al*[3,4] have focused on rigid transformation, denoted by τ (3 translation and 3 rotation parameters). The 3D CT scan is denoted by V. Several PI (n=2) are deduced from orthogonal viewpoints. The i^{th} PI is denoted by I_i, and the corresponding projection matrices (obtained with the calibration process) are denoted by Q_i. Given a similarity measure S, and I being the vector of n PI, the main 3D optimization procedure reveals:

$$\widetilde{\tau} = \arg\max_{\tau} S(QT(V), I) \tag{1}$$

In eq.1, $Q\tau(V)$ denotes a vector of n DRRs, according to n projection Q_i and patient displacement T. Every iteration of eq.1 requires the *on-line* generation of n DRRs. This process proves too lengthy to be easily tractable. We have attempted to elaborate a better solution to meet the time limitation.

2.2. Geometrical transformation approximation for DRR generation

We contemplated reducing the dimensional projections of space P by mainly considering out-of-plane rotations (2 parameters) and using in-plane (2D) transformations to retrieve the projection of QT. This decomposition assumes that 3D displacements are based on out-of-plane rotations. In theory this is however incorrect as the projection model is only a pinhole. Fortunately, the interval between the camera and the patient is much larger than the displacement amplitude of the patient and numerous experiments[3,4] have shown that this approximation is sufficient.

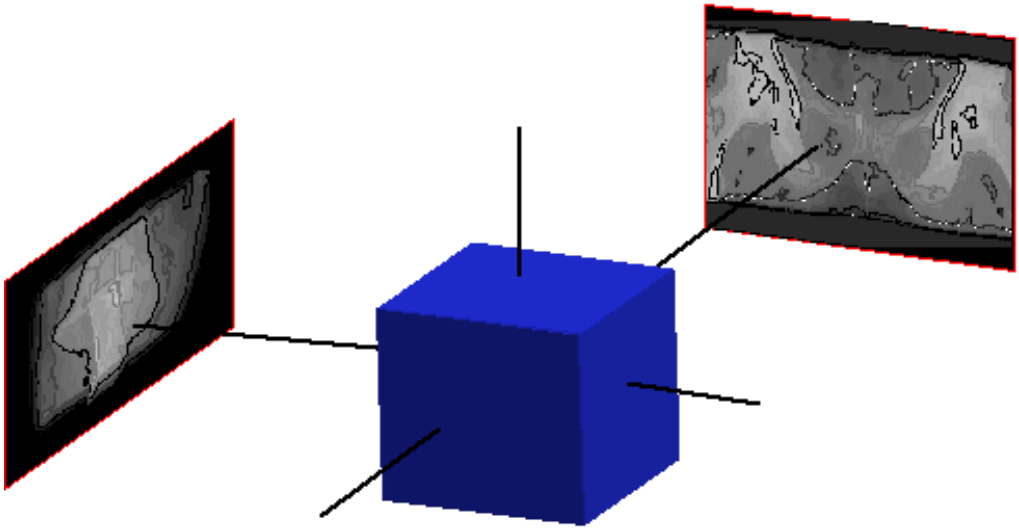

Figure 2. The patient displacement error is calculated by comparing 2 PIs with the 3D CT scan

Advantages The method is based on a rapid DRR generation algorithm that is an application of a 2D affine transformation of previously generated DRRs (obtained off-line prior to treatment). The set of pre-generated DRRs is built by sampling two out-of-plane rotations, which generously reduces the number of acquired DRRs for the registration process.

Drawbacks For a displacement interval of [-5°,+5°] and a half-degree precision, it is necessary to generate 900 DRRs per view per patient. The overall procedure computation time and disk space is highlighted in Table1. Increasing the degree of precision implies exponentially increasing the amount of pre-computed DRRs, thus

Nb of patients	Nb of DRRs	Computation time	Disk space
1	1800	30 mn	500 Mb
10	18000	10 h	5 Gb

Table 1.

hindering the real time implementation of the method for treatment. One proposed solution is to elaborate a DRR set off-line, then generate an online DRR that corresponds most precisely to patient displacement by interpolation from the DRR set. Next section introduces our work on the generation of artificial DRRs using the image morphing technique.

3. IMAGE MORPHING APPROACH FOR ARTIFICIAL DRR GENERATION

3.1. Digitally reconstructed radiographs (DRRs)

Definition A DRR is a computer-generated image of the bony anatomy as it would appear to a viewer located at the irradiation source and looking towards the isocenter. The figure described as follows is an example of a DRR generated starting from a scanner X of an anthromophic.

Generation DRRs are computed from the patient CT data with volume rendering, thus permitting to produce a virtual patient model (the DRRs that we generate are based on the ray tracing algorithm[5,6]). DRRs being digitalized, they can easily be managed by means of computer systems. However, the computing of images can be a time-consuming procedure, especially in the case of intensive use as required for 3D (scanner X) / 2D (PI) image registration. It is therefore crucial to devise a solution for the optimization of the generation process.

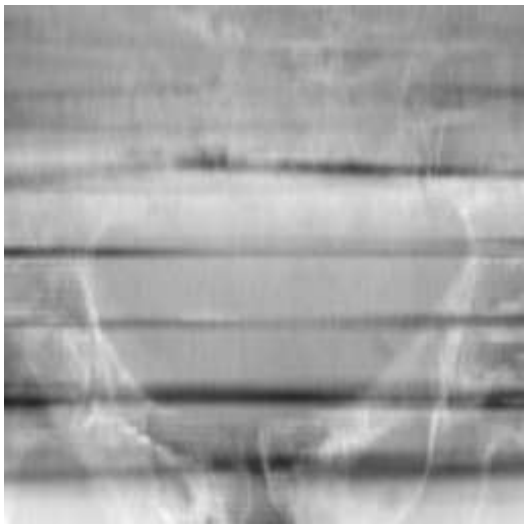

3.2. Stereo vision vs image morphing

The generation of virtual views from a pair of images has been a key issue in research during the last decade. It has brought about the emergence of two techniques: stereo vision and image morphing.

Stereo vision Stereo vision[7] can be defined as the reconstruction of the relief starting from several images of the same scene, viewed under various angles. Stereo vision involves three successive stages: calibration, mapping and triangulation. With stereovision, the generation of new images from other existing images, is a problem that strongly relates to the deduction of the three-dimensional structure of the scene. This particularity can be considered as a drawback, because the images have been inferred by the calibration process. For this reason, stereo vision was not adopted for DRR generation.

Image morphing Morphing between two images involves the deformation of reference images towards an intermediate selection, thus generating two intermediate images, followed by the application of a color blending technique (cross dissolve) to compute the final artificial image. Image morphing gives the flexibility for similarity between images and makes it possible to generate continuous deformations from source image to destination image. For this reason, image morphing was chosen as the basic technique for the generation of artificial DRRs.

3.3. Mesh warping

Numerous morphing techniques (mesh warping, field morphing, energy minimization, free-form deformations, etc) are available for the generation of artificial intermediate images. Generally, all these techniques follow similar procedures, and this includes establishing correspondences between images (via points, segments, curves, etc), calculating mapping functions, controlling transition and finally pixel interpolation (cross-dissolve). However, a simple, rapid, efficient and reliable morphing technique was desirable to investigate the feasibility of our approach (DRR generation via a morphing-based technique). For this initial platform, we have chosen to use mesh warping.[8]

In order to establish a correspondence between source and destination DRRs, we first developed a Graphical User Interface (GUI) from which we were able to map out a mesh of controlled coordinates regarding the characteristic spots of the source DRR (typically, the bone structures). The corresponding mesh for the destination DRR could be obtained by developing a block-matching algorithm[9] (cf. Fig 3). For this platform, we implemented the basic version of the block matching algorithm where an exhaustive search allows to determine the best match. Once both source and destination meshes had been computed and validated, the artificial intermediate DRR could be generated by using the mesh warping algorithm.

4. EXPERIMENTAL STUDIES

A series of tests were conducted to evaluate the quality of the DRRs generated by morphing as compared to reference DRRs, depending an the distance between source and destination DRRs, and on the number of in-between morphed DRRs to be generated.

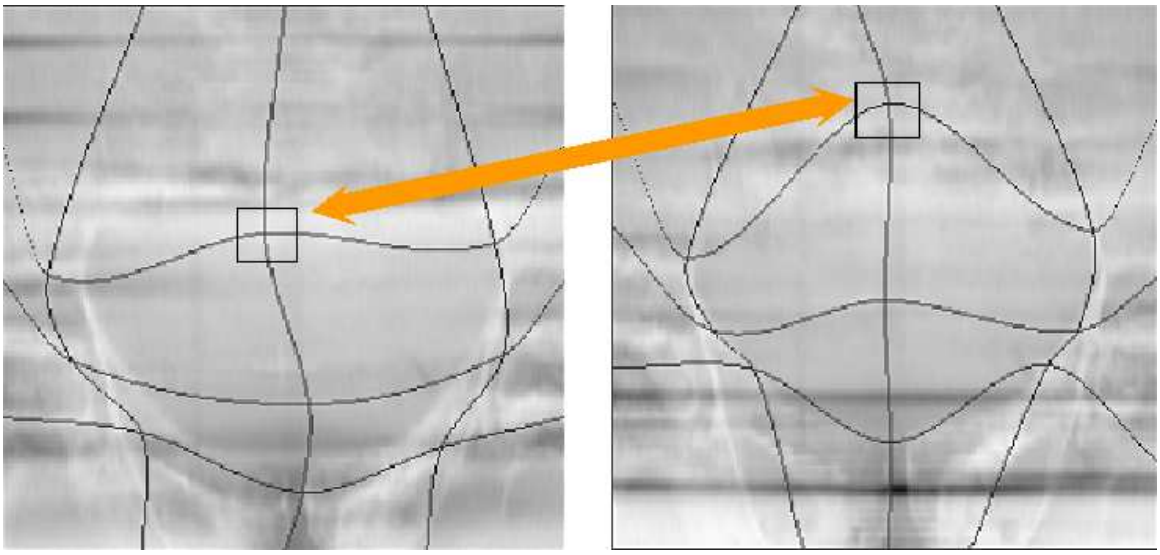

Figure 3. Illustration of the block matching algorithm

4.1. Material

We generated a series of DRRs while varying the horizontal rotation angle between -15° and +15°, and started generating morphed DRRs from the two most distant reference DRRs (at -15° and +15). Then, we continued generating other series of morphed images from less distant source and destination DRRs.

4.2. Methods and results

As the DRRs that we generate are intended to be used in a registration procedure, we evaluated them as follows:

- Initially, several basic tests (1^{st}, 2^{nd} and 3^{rd} tests) evaluated the quality of the DRRs generated by mesh warping.
- Secondly, we tried to determine whether morphed DRRs are accurate enough to replace reference DRRs (4^{th} test).

4.2.1. 1^{st} test: dissimilar evolution of morphed/reference DRR

We considered intervals starting from 4° up to 16° with a sampling step of 1°. Our first test simply consisted in comparing morphed DRRs with corresponding reference DRRs. The interval between source and destination DRRs is represented by the X axis, whereas a dissimilarity criterion (sum of absolute differences) is represented by the Y axis.

Whatever the interval taken, the curve keeps the same bell shape with a maximum dissimilarity for the middle DRR that varies from 1.98 gray level for 4° to 6.41 gray level for 16°. Moreover, we found that the longer the distance between the DRR to be generated and the reference source and destination DRRs, the worse the quality.

4.2.2. 2^{nd} test: dissimilar evolution of mid-morphed DRR and corresponding reference DRRs

Because it is located at an equal distance between source and destination DRRs, the mid-morphed DRR is contributed equally by reference source and destination DRRs, which may cause many problems in terms of quality when comparing to a reference DRR. Our second test consisted in calculating the dissimilarity between the in-between morphed DRR and the corresponding reference DRR at various intervals.

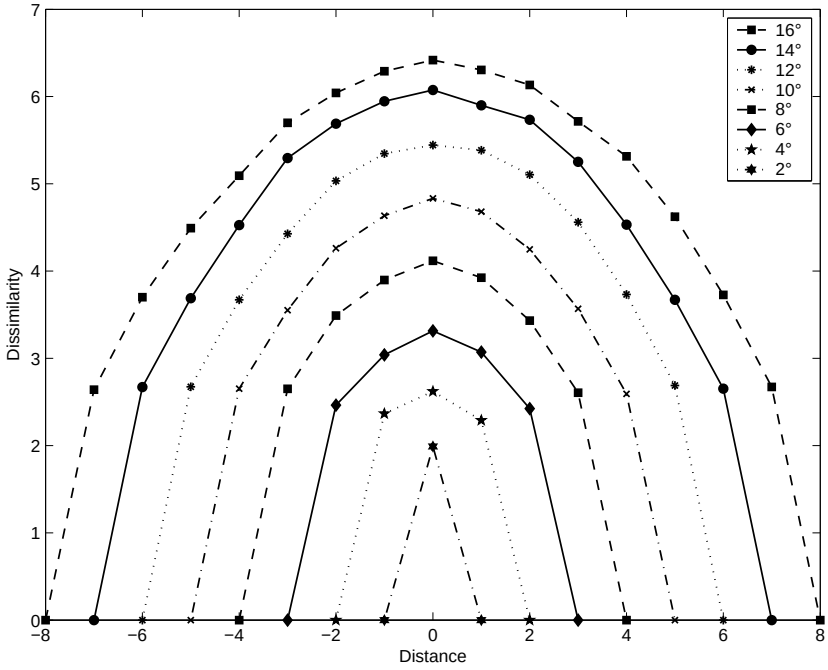

Figure 4. Dissimilarity between the morphed DRR and the reference DRRs according to the interval between reference source and destination DRRs

As expected, the longer the distance between the reference source and destination DRRs, the larger the dissimilarity between morphed and corresponding reference DRRs: about 1.42 gray level at a 2° interval (cf. Fig 5).

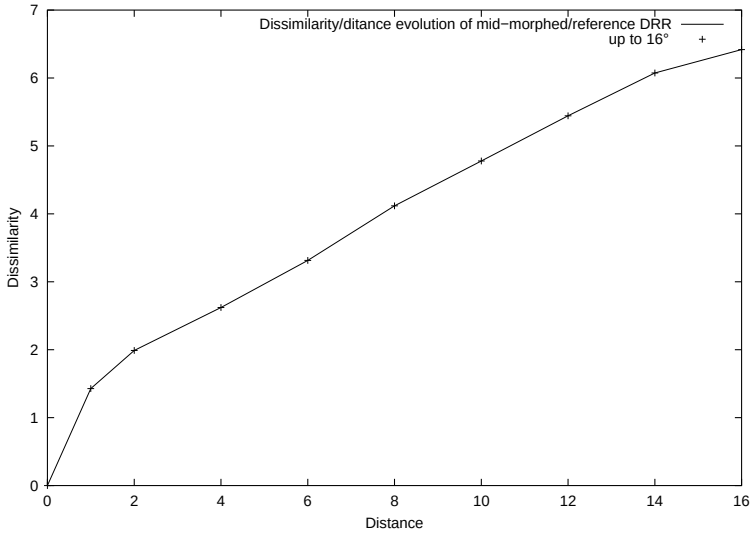

Figure 5. Dissimilarity/ditance evolution of mid-morphed to correspondent reference DRR

4.2.3. 3^{rd} test: mid-morphed DRR vs all reference DRRs

Our third test was to check whether the morphed DRR in the middle position (worst scenario) resembles more its corresponding reference DRR than all other DRRs in the set. In fact, when checked at reasonable

intervals (less than 6°), this assertion is valid (cf. Fig 6(a)), while it is not when intervals are larger, as shown in figure 6(b): in this case, the DRR generated with -1° shows a slightly lower dissimilarity than the expected 0° DRR.

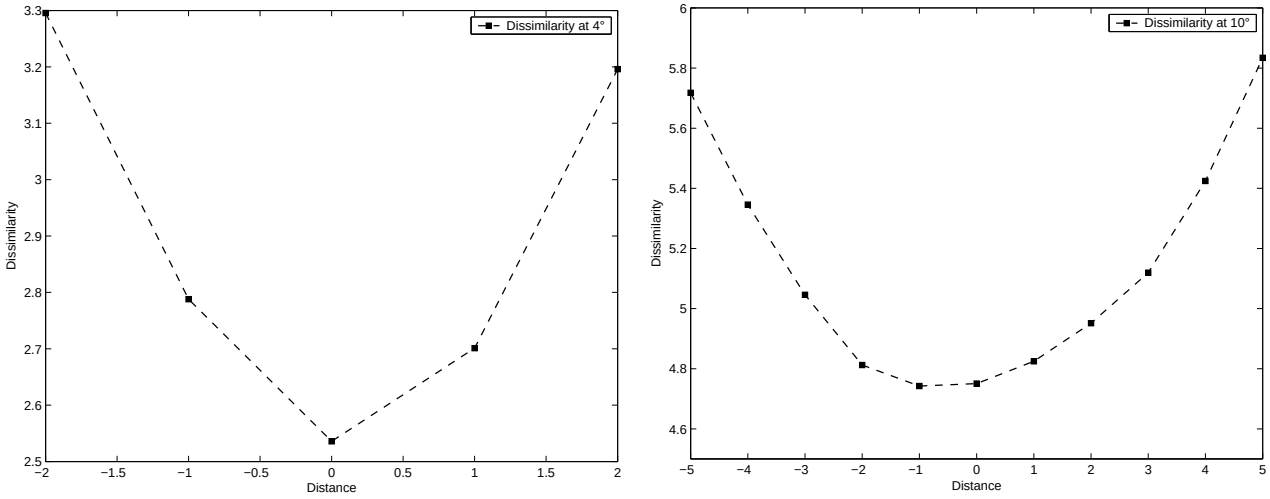

(a) 4° interval (b) 10° interval

Figure 6. Disimilarity of mid-morphed DRR to reference DRR

4.2.4. 4^{th} test: match between morphed and reference DRR

The fourth and final test consisted of comparing, as a function of the interval between source and destination DRRs and using the dissimilarity criterion, each morphed DRR with all reference DRRs in order to determine the best match. The ideal would be that each morphed DRR is more similar to its corresponding reference

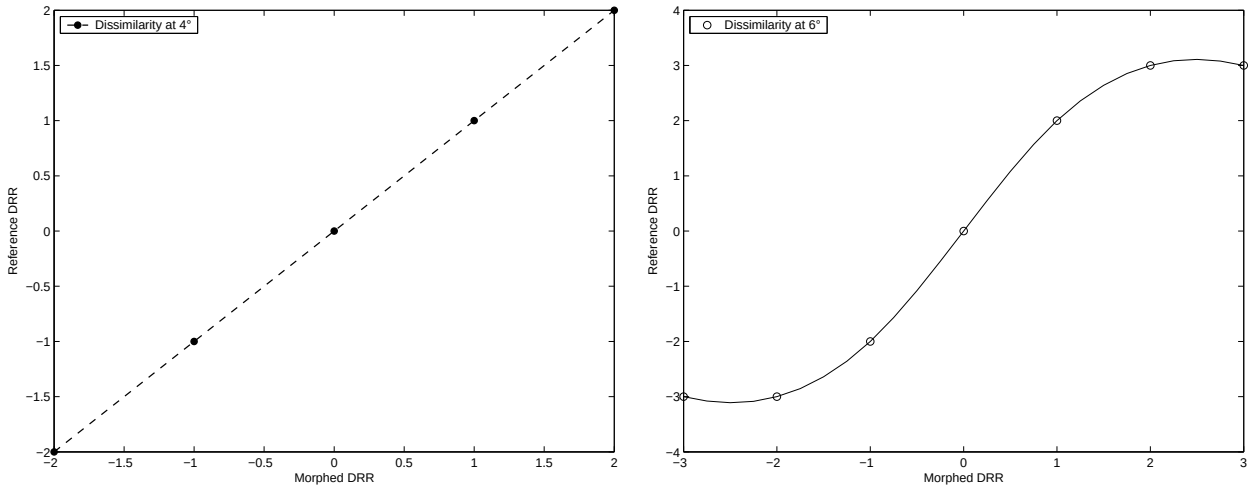

(a) 4° interval (b) 6° interval

Figure 7. Dissimilarity of morphed DRR to reference DRRs

DRR than to any other DRR in the set. Indeed, our assumption has been verified for interval lower than 4°, as shown in Figure 7(a).

However, for wider intervals, our assumption is no longer valid (c.f. Fig 7(b)). Therefore, there must be a trade-off between the interval size and the quality of the morphed DRR. Also, we believe that such an artefact is due to the cross-dissolve phase of the mesh warping where a simple linear interpolation is applied to calculate the pixels' gray level of intermediate DRR.

Even though, this is a very promising result, since it means that morphing-based DRR can be very useful in a registration procedures. From an off-line generated grid of DRRs, we can elaborate morphing-based DRRs by locally smoothening the grid via image morphing where necessary. This provides a high degree of precision without the need for an exponentially growing amount of costly DRRs (both in terms of computation time and disk space).

5. CONCLUSION AND FUTURE PROSPECTS

This paper introduces an original approach of DRR generation by 2D deformation (morphing). We believe that this is the first report of the use of morphing techniques for DRR generation in the context of conformal radiotherapy. The main strength of our method lies in the drastic cut in time necessary for DRR generation: 0.2 seconds per DRR with mesh morphing comparing to 2 seconds with ray tracing algorithm.

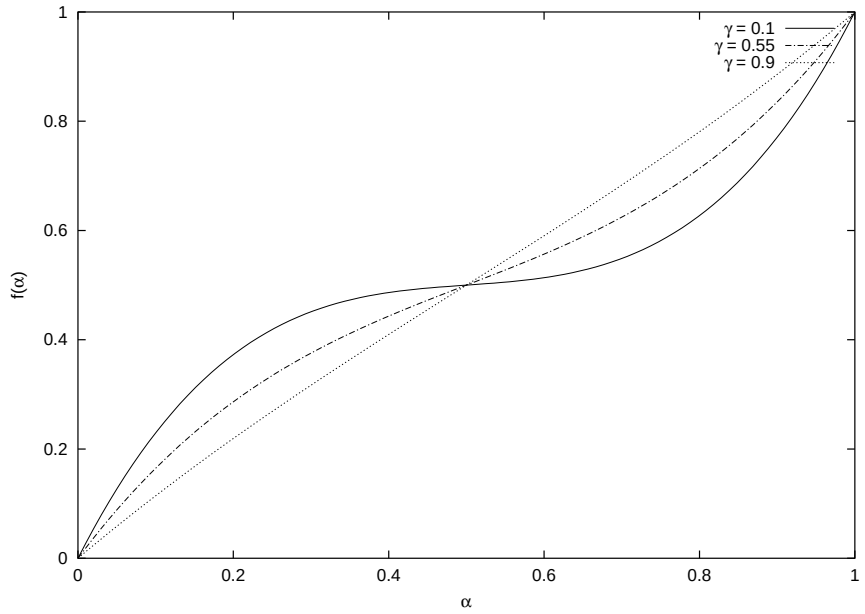

Figure 8. Cross-dissolve curve for various values of γ

Preliminary experiments show that morphed DRRs are accurate and can be used in registration procedures. Studies are ongoing to improve our method by automating the DRR mapping phase (by introducing an edge extraction process using snakes[10] as primitives) and replacing the *linear* cross-dissolve phase by a more adapted interpolation technique.

We believe that the main drawback of linear methods such as the cross-dissolve is that morphed DRRs are less influenced by the distance between corresponding source and destination DRRs. Indeed, morphed DRRs become more similar to reference DRRs close to the source or the destination DRRs than to their corresponding reference DRR. To overcome this artefact, the interpolation phase has to strengthen the contribution of distant reference DRRs to morphed DRRs. The curve of the interpolation parameter could be as follows: $f(\alpha) = 4(1-\gamma)(\alpha - \frac{1}{2})^3 + \gamma(\alpha - \frac{1}{2}) + \frac{1}{2}$ (cf. Fig 8).

REFERENCES

1. C. Carrie, S. Hoffstetter, and F. Gomez, "Impact of Targeting Deviations on Outcome in Medulloblastoma: Study of the French Society of Pediatric Oncology (SFOP).," *Int. J. Radiat. Oncol. Biol. Phys.* **45**, pp. 435–9, Sept. 1999.
2. P. Munro, "Portal Imaging Technology: Past, Present, and Future," *Sem. Radiat. Oncol.* **5**, pp. 115–133, 1995.
3. S. Clippe, D. Sarrut, C. Malet, S. Miguet, C. Ginestet, and C. Carrie, "Patient Setup Error Measurement Using 3D Intensity-Based Image Registration Techniques," *Int. J of Rad. Onco. Bio.Phys.* **56**(1), p. 259:265, 2003.
4. D. Sarrut and S. Clippe, "Geometrical Transformation Approximation for 2D/3D Intensity-Based Registration of Portal Images and CT Scan," in *Lecture Notes in Computer Science*, I. W. Niessen and e. M. A. Viergever, eds., **2208**, pp. 532–540, Medical Image Computing and Computer-Assisted Intervention MICCAI'2001, Springer Verlag, (Utrecht Netherlands), 2001.
5. J. Li and S. Miguet, "Parallel Volume Rendering of Medical Images," in *Ewpc'92: from theory to sound practice*, Q. Stout, ed., pp. 332–343, (Barcelone), 1992.
6. P. Lacroute, *Fast Volume Rendering Using a Shear-Warp Factorization of the Viewing Transformation.* PhD thesis, Stanford University, 1995.
7. D. Scharstein, *View Synthesis Using Stereo Vision*, Springer-Verlag, 1999.
8. G. Wolberg, *Digital Image Warping*, IEEE Computer Society Press, 1990.
9. E. Salari and W. Li, "Successive Elimination Algorithm For Motion Estimation," *IEEE transactions on image processing* **4**, pp. 105–107, January 1995.
10. M. Kass, A. WirthKin, and D. Trezopoulos, "Snakes: Active Contour Models," *Computer Vision* , pp. 321–331, 1998.